Supplement of

Projections of future hydrologic drought in a reservoir-regulated region: the role of climate change and reservoir operation

Shaokun He et al.

Correspondence to:

*Corresponding authors: chenkb@whu.edu.cn; ygong@whu.edu.cn

Contents of this file

Texts S1 to **S2**

Table S1

Figures S1 to **S5**

Text S1. Hyper-parameter tuning process of LSTM

Since the LSTM models were adopted with a three-layer structure and the input predictors were identified, the number of hidden nodes, the initial learning rate, and the dropout value of the LSTMs were the remaining hyper-parameters that needed to be determined. To this end, an enumeration method was used. In the enumeration, we first set the limited number of hidden nodes to {2, 3, 4, and 8}, the initial learning rate to {1×10^{-4}, 1×10^{-3}, and 5×10^{-3}}, the dropout value to {0, 0.1, 0.2, and 0.3}, respectively, and then conducted five independent experiments for each LSTM configuration to compare their average performance by consideration of the stochastic nature of LSTM simulations. The final experimental *NSE* results are shown in Table S1. The results show that most of the LSTM configurations achieve good performance on the daily-scale hydrological simulation. The performance differences between independent experiments are not significant, illustrating that LSTM is robust enough, although this is not elucidated in Table S1. After a comprehensive assessment and screening process, the 66th experiment (ID 66) was identified as the best performer. That is, the number of hidden nodes of LSTMs for reservoir inflow simulation and operating policy derivation is both 4, the initial learning rates are both 1×10^{-4}, and the dropout values are both 0.1.

In the performance evaluation of hydrological streamflow simulations of ID 66 at the monthly scale, the *NSE*s of reservoir inflow and release series are 0.93 and 0.91 during the calibration period, respectively; the percent bias (*PBIAS*) of the two series is 3.20% and 3.35%, respectively. The *NSE*s of inflow and release series are 0.95 and 0.89 during the validation period, respectively; the percent bias (*PBIAS*) is 0.29% and -3.35%, respectively. All the performances of ID 66 considerably exceed the hydrological modeling threshold (*NSE* greater than 0.50) proposed by Moriasi et al. (2007), which suggests that it is adequate for future streamflow projection.

Text S2. Optimization of reservoir operating policies

A multi-objective decision-making problem is formed for the Ankang reservoir and two metrics are considered: hydropower generation (i.e., total energy generated by the reservoir over the simulation period in units of kWh) and power generation guarantee rate (i.e., ratio of the number of times over the simulation period that the monthly average power output is greater than the guarantee power to the total number of time periods). For medium- and long-term hydropower operations of reservoirs, these two metrics are commonly used to measure the operation performance (Chen et al., 2019; Li et al., 2022; Si et al., 2018), which can be expressed by Equations (S1) and (S2).

$$max\ f_{THP} = \sum_{t=1}^{T} \frac{P_t \cdot (\Delta t / 3600)}{Y}, \quad P_t = k \cdot H_t \cdot QG_t \qquad \text{(S1)}$$

$$max\ f_{PGR} = \sum_{t=1}^{T} \Lambda / T * 100\%, \Lambda = \begin{cases} 0 & if\ P_t < P_{gua} \\ 1 & else \end{cases} \qquad \text{(S2)}$$

where P_t (kW) = electric power generated by the reservoir at time t; k = efficiency coefficient of the reservoir, which is assumed to be constant over time; H_t (m) = hydraulic head at time t; QG_t (m^3/s) = water release for hydropower generation at time t; f_{THP} (kW·h) = total hydropower production (i.e., annual average energy output); Δt (s) = numerical discretization time step; Y = total number of years in the simulation periods; t = 1, 2, …, T, and T = total number of simulation periods; f_{PGR} = power generation guarantee rate; Λ = Boolean variable (i.e., 0 or 1), 0 when P_t is less than the guaranteed power and 1 otherwise.

Additionally, reservoir operation optimization should obey the following constraints:

$$V_{t+1} = V_t + (I_t - O_t) \cdot \Delta t \qquad \text{(S3)}$$

$$V_{min} \le V_t \le V_{max} \qquad \text{(S4)}$$

$$O_{min} \le O_t \le O_{max},\ O_t = QG_t + QS_t \qquad \text{(S5)}$$

$$P_{min} \le P_t \le P_{max} \qquad \text{(S6)}$$

where Equations (S3) - (S5) are the same as Equations (6) – (8) in the text. QS_t (m^3/s) = spill flow at time t; P_{min} (kW) and P_{max} (kW) are the allowable minimum and maximum power outputs, respectively.

We subsequently represent the operating policies with Gaussian radial basis functions (RBFs) due to their reported positive scalability with respect to the state-decision space (Yang et al., 2020; Quinn et al., 2017). The RBF-based policy representation is expressed in Equation (S7), where u_t is the policy-designated reservoir release at time *t* (normalized to [0, 1]), $(X_t)_m$ is the value of the *m*th of M time-varying inputs at time *t* (normalized to [0, 1]), and w_k, $c_{k,m}$, and b_k are the weights, centers, and radii of RBFs, respectively.

$$u_t = \sum_{k=1}^{K} w_k \exp\left[-\sum_{m=1}^{M} \frac{((X_t)_m - c_{k,m})^2}{b_k} \right] \tag{S7}$$

where $w_k \in [0,1]$ with $\sum_{k=1}^{K} w_k = 1$, $c_{k,m} \in [-1,1]$, and $b_{k,m} \in (0,1]$. We modeled reservoir releases using three inputs: current reservoir storage, current reservoir inflow, and time of year, as suggested by Yang et al. (2017) for this reservoir system. Notably, the final true release at time *t* may not always be equal to the unnormalized policy-designated release at time *t* due to physical release constraints. If there is insufficient reservoir storage capacity to allow a release of only the unnormalized magnitude of u_t, the excess is spilled, and if there is less water than the unnormalized u_t, only the available water is released.

Finally, the nondominated sorting genetic algorithm version 2 (NSGA-II) (Deb et al., 2002) is used to optimize the policy parameters, with hyperparameter values of 100 and 1000 for the population size and number of generations, respectively. The resulting Pareto front π_θ^* is presented in Figure S5.

Table S1. The average *Nash-Sutcliffe* (*NSE*) performance of LSTM in the daily hydrological simulation with different hyper-parameter combinations.

Experiment ID	Hidden_size	End_lr	Hidden_ channel	dropout	Calibration period (1993-2014)		Validation period (2015-2020)	
					Inflow	Release	Inflow	Release
1	8	0.005	8	0	0.864	0.802	0.736	0.651
2	8	0.001	8	0	0.862	0.797	0.733	0.649
3	8	1.00E-04	8	0	0.862	0.804	0.733	0.64
4	8	0.005	8	0.1	0.857	0.799	0.74	0.659
5	8	0.001	8	0.1	0.855	0.792	0.736	0.656
6	8	1.00E-04	8	0.1	0.853	0.785	0.735	0.652
7	8	0.005	8	0.2	0.853	0.79	0.741	0.659
8	8	0.001	8	0.2	0.852	0.785	0.741	0.657
9	8	1.00E-04	8	0.2	0.853	0.783	0.744	0.657
10	8	0.005	8	0.3	0.851	0.789	0.747	0.661
11	8	0.001	8	0.3	0.851	0.784	0.746	0.658
12	8	1.00E-04	8	0.3	0.847	0.782	0.741	0.656
13	8	0.005	4	0	0.856	0.805	0.729	0.646
14	8	0.001	4	0	0.853	0.8	0.72	0.641
15	8	1.00E-04	4	0	0.854	0.8	0.726	0.648
16	8	0.005	4	0.1	0.854	0.794	0.739	0.669
17	8	0.001	4	0.1	0.853	0.788	0.739	0.676
18	8	1.00E-04	4	0.1	0.852	0.791	0.736	0.666
19	8	0.005	4	0.2	0.849	0.79	0.743	0.678
20	8	0.001	4	0.2	0.849	0.792	0.744	0.67
21	8	1.00E-04	4	0.2	0.847	0.792	0.742	0.668
22	8	0.005	4	0.3	0.833	0.756	0.735	0.684
23	8	0.001	4	0.3	0.835	0.777	0.742	0.673
24	8	1.00E-04	4	0.3	0.836	0.772	0.736	0.675
25	8	0.005	3	0	0.849	0.794	0.711	0.638
26	8	0.001	3	0	0.847	0.795	0.706	0.62
27	8	1.00E-04	3	0	0.843	0.789	0.703	0.625
28	8	0.005	3	0.1	0.852	0.799	0.738	0.673
29	8	0.001	3	0.1	0.852	0.794	0.737	0.671
30	8	1.00E-04	3	0.1	0.851	0.792	0.737	0.663
31	8	0.005	3	0.2	0.843	0.787	0.74	0.679
32	8	0.001	3	0.2	0.841	0.783	0.735	0.678
33	8	1.00E-04	3	0.2	0.837	0.767	0.734	0.681
34	8	0.005	3	0.3	0.833	0.77	0.74	0.685
35	8	0.001	3	0.3	0.828	0.761	0.73	0.678
36	8	1.00E-04	3	0.3	0.827	0.756	0.735	0.683
37	8	0.005	2	0	0.85	0.798	0.714	0.639
38	8	0.001	2	0	0.849	0.8	0.712	0.619
39	8	1.00E-04	2	0	0.848	0.8	0.709	0.617

40	8	0.005	2	0.1	0.841	0.748	0.726	0.682
41	8	0.001	2	0.1	0.844	0.78	0.724	0.663
42	8	1.00E-04	2	0.1	0.844	0.779	0.727	0.657
43	8	0.005	2	0.2	0.831	0.763	0.733	0.68
44	8	0.001	2	0.2	0.827	0.755	0.731	0.676
45	8	1.00E-04	2	0.2	0.828	0.758	0.73	0.677
46	8	0.005	2	0.3	0.809	0.764	0.725	0.67
47	8	0.001	2	0.3	0.808	0.758	0.73	0.67
48	8	1.00E-04	2	0.3	0.809	0.756	0.73	0.669
49	4	0.005	8	0	0.862	0.8	0.737	0.661
50	4	0.001	8	0	0.864	0.806	0.736	0.655
51	4	1.00E-04	8	0	0.864	0.804	0.734	0.653
52	4	0.005	8	0.1	0.852	0.798	0.754	0.658
53	4	0.001	8	0.1	0.856	0.802	0.742	0.649
54	4	1.00E-04	8	0.1	0.855	0.795	0.741	0.654
55	4	0.005	8	0.2	0.855	0.795	0.74	0.661
56	4	0.001	8	0.2	0.853	0.792	0.747	0.658
57	4	1.00E-04	8	0.2	0.855	0.798	0.751	0.65
58	4	0.005	8	0.3	0.845	0.784	0.748	0.661
59	4	0.001	8	0.3	0.844	0.786	0.743	0.654
60	4	1.00E-04	8	0.3	0.845	0.788	0.746	0.649
61	4	0.005	4	0	0.862	0.799	0.73	0.649
62	4	0.001	4	0	0.862	0.799	0.731	0.642
63	4	1.00E-04	4	0	0.861	0.802	0.725	0.637
64	4	0.005	4	0.1	0.854	0.8	0.742	0.657
65	4	0.001	4	0.1	0.856	0.802	0.744	0.649
66	**4**	**1.00E-04**	**4**	**0.1**	**0.851**	**0.793**	**0.74**	**0.65**
67	4	0.005	4	0.2	0.847	0.774	0.739	0.692
68	4	0.001	4	0.2	0.844	0.781	0.742	0.661
69	4	1.00E-04	4	0.2	0.846	0.787	0.742	0.663
70	4	0.005	4	0.3	0.835	0.777	0.743	0.665
71	4	0.001	4	0.3	0.835	0.78	0.735	0.661
72	4	1.00E-04	4	0.3	0.833	0.776	0.742	0.663
73	4	0.005	3	0	0.848	0.793	0.698	0.63
74	4	0.001	3	0	0.85	0.796	0.708	0.621
75	4	1.00E-04	3	0	0.85	0.793	0.707	0.624
76	4	0.005	3	0.1	0.849	0.796	0.74	0.67
77	4	0.001	3	0.1	0.848	0.797	0.733	0.658
78	4	1.00E-04	3	0.1	0.847	0.793	0.734	0.656
79	4	0.005	3	0.2	0.835	0.764	0.732	0.677
80	4	0.001	3	0.2	0.836	0.78	0.737	0.669
81	4	1.00E-04	3	0.2	0.834	0.773	0.737	0.668
82	4	0.005	3	0.3	0.825	0.765	0.734	0.673
83	4	0.001	3	0.3	0.822	0.764	0.731	0.67
84	4	1.00E-04	3	0.3	0.822	0.766	0.734	0.668

85	4	0.005	2	0	0.847	0.802	0.708	0.627
86	4	0.001	2	0	0.846	0.801	0.705	0.619
87	4	1.00E-04	2	0	0.845	0.8	0.704	0.622
88	4	0.005	2	0.1	0.843	0.775	0.735	0.656
89	4	0.001	2	0.1	0.842	0.781	0.732	0.658
90	4	1.00E-04	2	0.1	0.845	0.788	0.733	0.65
91	4	0.005	2	0.2	0.831	0.767	0.734	0.669
92	4	0.001	2	0.2	0.827	0.762	0.73	0.66
93	4	1.00E-04	2	0.2	0.825	0.766	0.73	0.658
94	4	0.005	2	0.3	0.803	0.738	0.725	0.671
95	4	0.001	2	0.3	0.801	0.738	0.722	0.666
96	4	1.00E-04	2	0.3	0.799	0.733	0.722	0.663
97	3	0.005	8	0	0.866	0.803	0.744	0.653
98	3	0.001	8	0	0.866	0.806	0.737	0.641
99	3	1.00E-04	8	0	0.865	0.806	0.735	0.64
100	3	0.005	8	0.1	0.858	0.803	0.746	0.667
101	3	0.001	8	0.1	0.856	0.8	0.748	0.669
102	3	1.00E-04	8	0.1	0.853	0.791	0.743	0.656
103	3	0.005	8	0.2	0.856	0.797	0.75	0.667
104	3	0.001	8	0.2	0.852	0.795	0.748	0.659
105	3	1.00E-04	8	0.2	0.855	0.799	0.748	0.654
106	3	0.005	8	0.3	0.843	0.781	0.748	0.66
107	3	0.001	8	0.3	0.847	0.79	0.749	0.648
108	3	1.00E-04	8	0.3	0.847	0.794	0.749	0.651
109	3	0.005	4	0	0.859	0.794	0.737	0.656
110	3	0.001	4	0	0.861	0.803	0.73	0.644
111	3	1.00E-04	4	0	0.862	0.806	0.732	0.638
112	3	0.005	4	0.1	0.855	0.801	0.749	0.667
113	3	0.001	4	0.1	0.851	0.796	0.746	0.669
114	3	1.00E-04	4	0.1	0.855	0.801	0.746	0.662
115	3	0.005	4	0.2	0.848	0.792	0.745	0.669
116	3	0.001	4	0.2	0.846	0.794	0.75	0.667
117	3	1.00E-04	4	0.2	0.845	0.791	0.746	0.669
118	3	0.005	4	0.3	0.835	0.78	0.744	0.662
119	3	0.001	4	0.3	0.832	0.779	0.743	0.67
120	3	1.00E-04	4	0.3	0.828	0.777	0.736	0.668
121	3	0.005	3	0	0.857	0.796	0.727	0.66
122	3	0.001	3	0	0.859	0.805	0.725	0.641
123	3	1.00E-04	3	0	0.856	0.798	0.727	0.641
124	3	0.005	3	0.1	0.851	0.797	0.747	0.663
125	3	0.001	3	0.1	0.849	0.788	0.745	0.666
126	3	1.00E-04	3	0.1	0.851	0.801	0.743	0.66
127	3	0.005	3	0.2	0.843	0.787	0.749	0.67
128	3	0.001	3	0.2	0.841	0.788	0.748	0.663
129	3	1.00E-04	3	0.2	0.842	0.792	0.747	0.659

130	3	0.005	3	0.3	0.825	0.766	0.743	0.666
131	3	0.001	3	0.3	0.825	0.77	0.74	0.65
132	3	1.00E-04	3	0.3	0.828	0.776	0.742	0.655
133	3	0.005	2	0	0.851	0.797	0.716	0.63
134	3	0.001	2	0	0.846	0.796	0.708	0.618
135	3	1.00E-04	2	0	0.848	0.794	0.712	0.628
136	3	0.005	2	0.1	0.848	0.781	0.739	0.664
137	3	0.001	2	0.1	0.846	0.783	0.738	0.658
138	3	1.00E-04	2	0.1	0.846	0.784	0.737	0.667
139	3	0.005	2	0.2	0.834	0.78	0.744	0.662
140	3	0.001	2	0.2	0.83	0.772	0.737	0.661
141	3	1.00E-04	2	0.2	0.83	0.765	0.734	0.66
142	3	0.005	2	0.3	0.807	0.743	0.731	0.666
143	3	0.001	2	0.3	0.806	0.742	0.726	0.667
144	3	1.00E-04	2	0.3	0.802	0.736	0.723	0.662
145	2	0.005	8	0	0.862	0.798	0.741	0.659
146	2	0.001	8	0	0.864	0.805	0.734	0.638
147	2	1.00E-04	8	0	0.863	0.802	0.739	0.642
148	2	0.005	8	0.1	0.857	0.802	0.748	0.65
149	2	0.001	8	0.1	0.858	0.8	0.748	0.651
150	2	1.00E-04	8	0.1	0.855	0.799	0.746	0.657
151	2	0.005	8	0.2	0.853	0.79	0.748	0.659
152	2	0.001	8	0.2	0.855	0.796	0.75	0.655
153	2	1.00E-04	8	0.2	0.852	0.799	0.746	0.653
154	2	0.005	8	0.3	0.846	0.784	0.748	0.645
155	2	0.001	8	0.3	0.843	0.782	0.75	0.636
156	2	1.00E-04	8	0.3	0.847	0.788	0.749	0.638
157	2	0.005	4	0	0.861	0.8	0.732	0.654
158	2	0.001	4	0	0.861	0.806	0.732	0.649
159	2	1.00E-04	4	0	0.86	0.805	0.729	0.643
160	2	0.005	4	0.1	0.85	0.789	0.741	0.664
161	2	0.001	4	0.1	0.855	0.804	0.74	0.66
162	2	1.00E-04	4	0.1	0.853	0.8	0.741	0.66
163	2	0.005	4	0.2	0.842	0.786	0.74	0.66
164	2	0.001	4	0.2	0.839	0.772	0.737	0.649
165	2	1.00E-04	4	0.2	0.844	0.791	0.744	0.644
166	2	0.005	4	0.3	0.832	0.778	0.742	0.656
167	2	0.001	4	0.3	0.829	0.773	0.736	0.64
168	2	1.00E-04	4	0.3	0.829	0.775	0.737	0.653
169	2	0.005	3	0	0.857	0.806	0.716	0.625
170	2	0.001	3	0	0.852	0.8	0.712	0.623
171	2	1.00E-04	3	0	0.851	0.801	0.707	0.613
172	2	0.005	3	0.1	0.849	0.801	0.756	0.661
173	2	0.001	3	0.1	0.855	0.801	0.741	0.655
174	2	1.00E-04	3	0.1	0.855	0.8	0.742	0.66

175	2	0.005	3	0.2	0.841	0.785	0.752	0.665
176	2	0.001	3	0.2	0.838	0.785	0.744	0.661
177	2	1.00E-04	3	0.2	0.841	0.785	0.746	0.665
178	2	0.005	3	0.3	0.819	0.767	0.737	0.654
179	2	0.001	3	0.3	0.819	0.767	0.733	0.647
180	2	1.00E-04	3	0.3	0.819	0.766	0.74	0.652
181	2	0.005	2	0	0.844	0.799	0.693	0.615
182	2	0.001	2	0	0.846	0.799	0.706	0.618
183	2	1.00E-04	2	0	0.846	0.799	0.705	0.615
184	2	0.005	2	0.1	0.838	0.783	0.723	0.663
185	2	0.001	2	0.1	0.841	0.792	0.72	0.649
186	2	1.00E-04	2	0.1	0.837	0.789	0.717	0.643
187	2	0.005	2	0.2	0.824	0.768	0.718	0.66
188	2	0.001	2	0.2	0.821	0.772	0.719	0.652
189	2	1.00E-04	2	0.2	0.822	0.773	0.723	0.659
190	2	0.005	2	0.3	0.803	0.755	0.715	0.652
191	2	0.001	2	0.3	0.793	0.741	0.707	0.649
192	2	1.00E-04	2	0.3	0.798	0.749	0.713	0.649

98

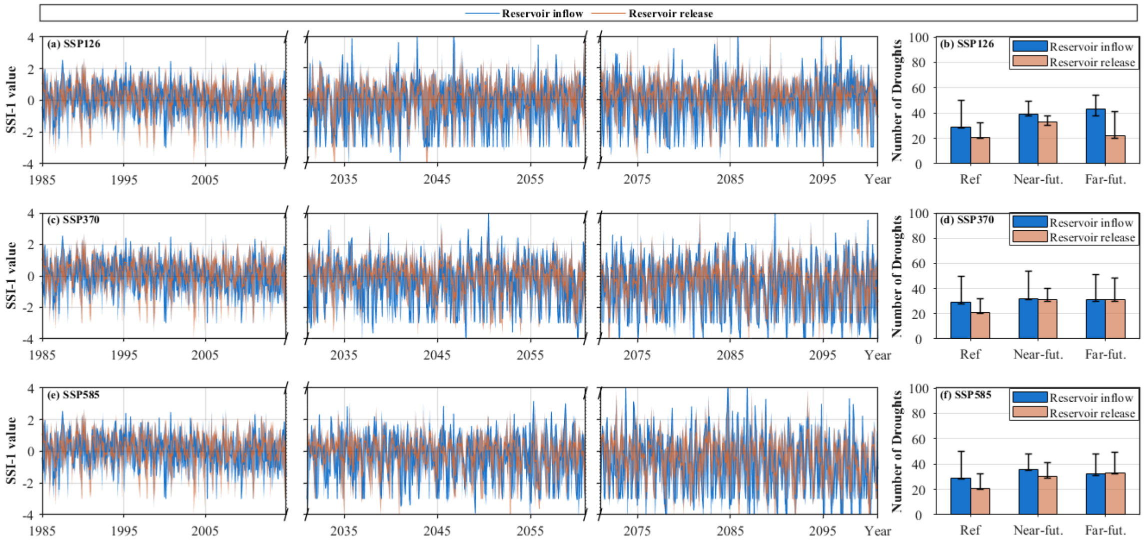

Figure S1. Hydrological drought SSI-1 for reference and future periods over the UHRB. (a) Time series of SSI-1 associated with reservoir inflow and release for the low-emission SSP126 scenario. Blue and orange intervals indicate their uncertainties, respectively. (b) Number of drought events for the reference period (1985–2014), near-future period (2031–2060), and far-future period (2071–2100). Colored bars are ensemble means and error bars represent the estimated difference in the number of drought events among the five GCMs. (c-d) is the same as (a-b), but for the medium-emission SSP370 scenario. (e-f) is the same as (a-b), but for the high-emission SSP585 scenario.

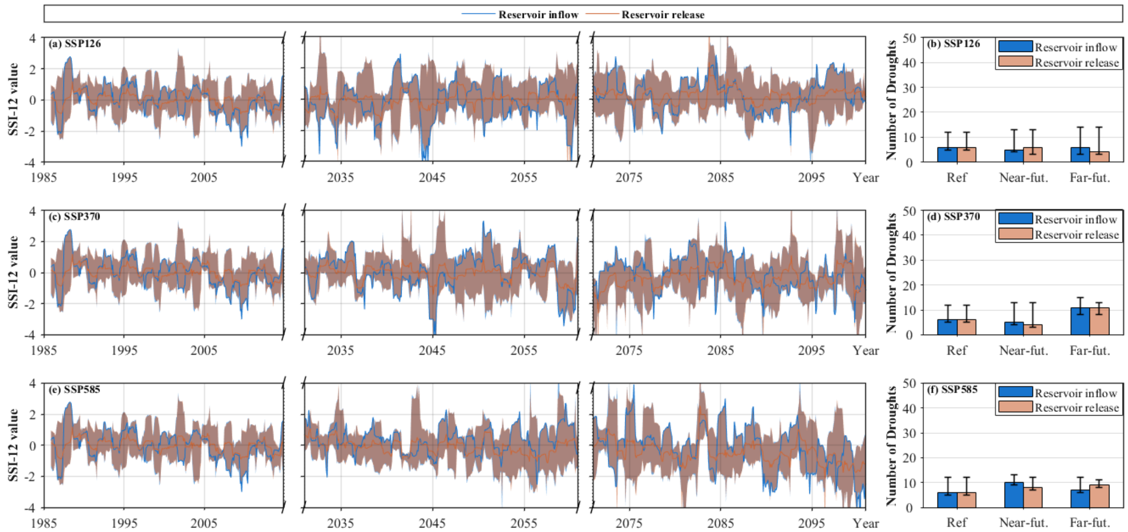

Figure S2. Hydrological drought SSI-12 for reference and future periods over the UHRB. (a) Time series of SSI-12 associated with reservoir inflow and release for the low-emission SSP126 scenario. Blue and orange intervals indicate their uncertainties, respectively. (b) Number of drought events for the reference period (1985–2014), near-future period (2031–2060), and far-future period (2071–2100). Colored bars are ensemble means and error bars represent the estimated difference in the number of drought events among the five GCMs. (c-d) is the same as (a-b), but for the medium-emission SSP370 scenario. (e-f) is the same as (a-b), but for the high-emission SSP585 scenario.

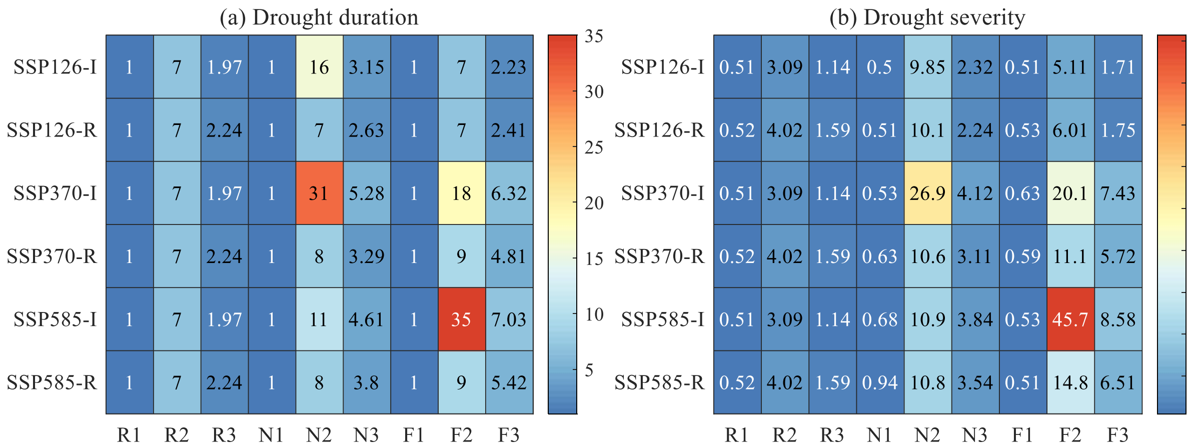

Figure S3. Heat map representation of (a) drought duration and (b) drought severity for the GCM-averaged SSI-1 series. The symbols R1, R2 and R3 indicate the minimum, maximum, and mean values during the reference period (1985–2014). N1, N2 and N3 are the same, but for the near-future period (2031–2060). F1, F2, and F3 are for the far-future period (2071–2100). Additionally, SSP126-I and SSP126-R are associated with reservoir inflow and release in the SSP126 scenario, SSP370-I and SSP370-R with the SSP370 scenario, and SSP585-I and SSP585-R with the SSP585 scenario.

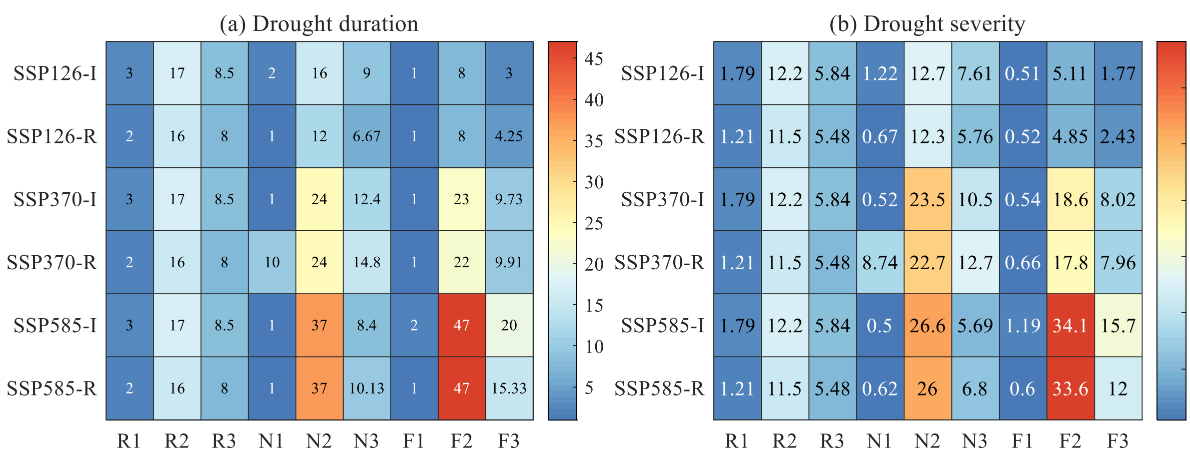

Figure S4. Heat map representation of (a) drought duration and (b) drought severity for the GCM-averaged SSI-12 series. The symbols R1, R2 and R3 indicate the minimum, maximum, and mean values during the reference period (1985–2014). N1, N2 and N3 are the same, but for the near-future period (2031–2060). F1, F2, and F3 are for the far-future period (2071–2100). Additionally, SSP126-I and SSP126-R are associated with reservoir inflow and release in the SSP126 scenario, SSP370-I and SSP370-R with the SSP370 scenario, and SSP585-I and SSP585-R with the SSP585 scenario.

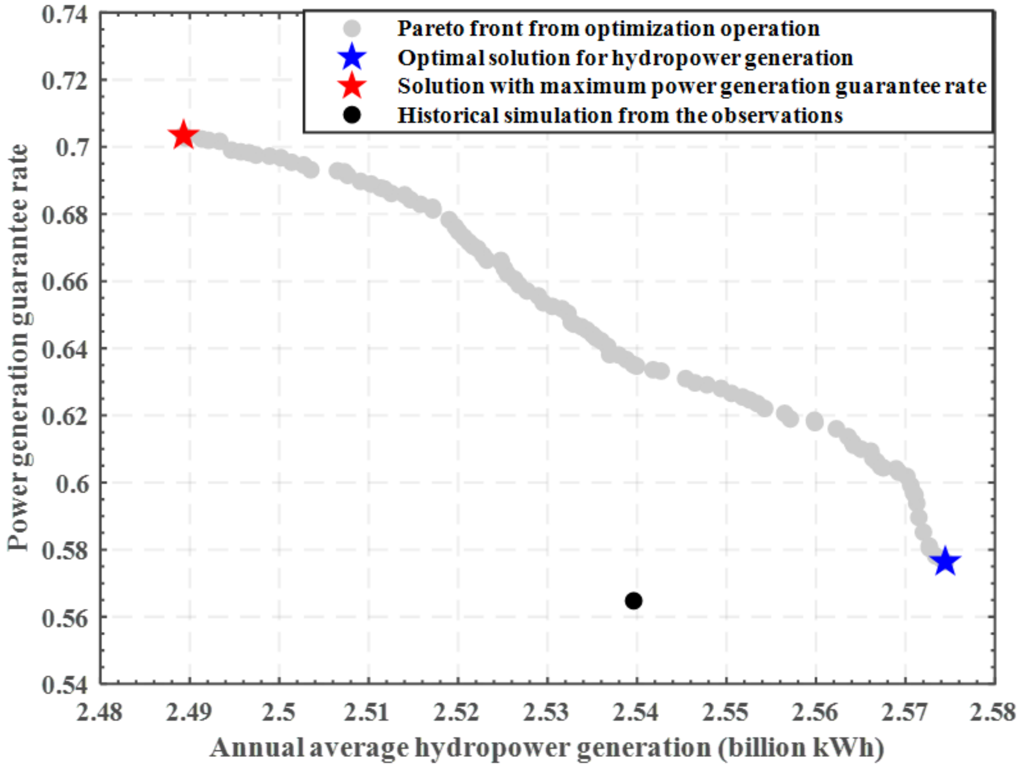

Figure S5. Trade-off between annual average hydropower generation and power generation guarantee rate for the Ankang Reservoir. Each grey dot represents an optimal operating policy identified using the NSGA-II algorithm, forming the Pareto front. The blue star marks the solution with the maximum hydropower generation, while the red star indicates the solution with the highest power generation guarantee rate. The black dot represents the historical operation derived from observed records.

References

Chen, X., Xu, B., Zheng, Y., and Zhang, C.: Nexus of water, energy and ecosystems in the upper Mekong River: A system analysis of phosphorus transport through cascade reservoirs, Sci Total Environ, 671, 1179-1191, 10.1016/j.scitotenv.2019.03.324, 2019.

Deb, K., Pratap, A., Agarwal, S., and Meyarivan, T.: A fast and elitist multiobjective genetic algorithm: NSGA-II, Ieee T Evolut Comput, 6, 182-197, 10.1109/4235.996017, 2002.

Li, X., Liu, P., Wang, Y., Yang, Z., Gong, Y., An, R., Huang, K., and Wen, Y.: Derivation of operating rule curves for cascade hydropower reservoirs considering the spot market: A case study of the China's Qing River cascade-reservoir system, Renewable Energy, 182, 1028-1038, 10.1016/j.renene.2021.11.013, 2022.

Moriasi, D. N., Arnold, J. G., Van Liew, M. W., Bingner, R. L., Harmel, R. D., and Veith, T. L.: Model evaluation guidelines for systematic quantification of accuracy in watershed simulations, T Asabe, 50, 885-900, 10.13031/2013.23153, 2007.

Quinn, J. D., Reed, P. M., Giuliani, M., and Castelletti, A.: Rival framings: A framework for discovering how problem formulation uncertainties shape risk management trade - offs in water resources systems, Water Resour Res, 53, 7208-7233, 10.1002/2017wr020524, 2017.

Si, Y., Li, X., Yin, D., Liu, R., Wei, J., Huang, Y., Li, T., Liu, J., Gu, S., and Wang, G.: Evaluating and optimizing the operation of the hydropower system in the Upper Yellow River: A general LINGO-based integrated framework, Plos One, 13, e0191483, 10.1371/journal.pone.0191483, 2018.

Yang, G., Guo, S. L., Liu, P., and Block, P.: Integration and evaluation of forecast-informed multiobjective reservoir operations, J Water Res Plan Man, 146, 04020038, 10.1061/(Asce)Wr.1943-5452.0001229, 2020.

Yang, G., Guo, S. L., Liu, P., Li, L. P., and Xu, C. Y.: Multiobjective reservoir operating rules based on cascade reservoir input variable selection method, Water Resour Res, 53, 3446-3463, 10.1002/2016wr020301, 2017.